Available online at www.sciencedirect.com
ScienceDirect
Carbohydrate Research 342 (2007) 717–723
Carbohydrate RESEARCH

Aleppo tannin: structural analysis and salivary amylase inhibition

Ágnes Zajácz,[a] Gyöngyi Gyémánt,[a] Natale Vittori[b] and Lili Kandra[a,*]

[a]*University of Debrecen, Faculty of Sciences, Department of Biochemistry, PO Box 55, H-4010 Debrecen, Hungary*
[b]*Biotechnology Services and Consulting Inc., 517 Parkway Boulevard, Coppell, TX 75019, USA*

Received 25 May 2006; received in revised form 18 December 2006; accepted 19 December 2006
Available online 22 December 2006

Abstract—The effectiveness and specificity of a tannin inhibition on human salivary amylase (HSA) catalyzed hydrolysis was studied using 2-chloro-4-nitrophenyl 4-*O*-β-D-galactopyranosyl-α-maltoside ($GalG_2$-CNP) and amylose substrates. Aleppo tannin was isolated from the gall nut of Aleppo oak. This tannin is a gallotannin, in which glucose is esterified with gallic acids. This is the first kinetic report, which details the inhibitory effects of this compound on HSA. A mixed non-competitive type inhibition has been observed on both substrates. The extent of inhibition is markedly dependent on the substrate-type. Kinetic constants were calculated from Lineweaver–Burk secondary plots for $GalG_2$-CNP (K_{EI} 0.82 μg mL^{-1}, K_{ESI} 3.3 μg mL^{-1}). This indicates a 1:1 binding ratio of inhibitor–enzyme and/or inhibitor–enzyme–substrate complex. When amylose was the substrate the binding ratio of inhibitor to enzyme–substrate complex was found to be 2:1, with the binding constants of K_{EI} 17.4 μg mL^{-1}, K_{ESI} 14.9 μg mL^{-1}, K_{ESI_2} 9.6 μg mL^{-1}. Presumably, the tannin inhibitor can bind not only to HSA, but to the amylose substrate, as well. Kinetic data suggest that Aleppo tannin is a more efficient amylase inhibitor than the recently studied other tannin with quinic acid core ($GalG_2$-CNP: K_{EI} 9.0 μg mL^{-1}, K_{ESI} 47.9 μg mL^{-1}).
© 2006 Elsevier Ltd. All rights reserved.

Keywords: HSA; Inhibitor; Kinetic analysis; Aleppo tannin; Gallotannin

1. Introduction

Interactions between salivary components and bacteria are thought to be important with regards to oral microflora, which play a crucial role in the formation of oral diseases, including dental caries, periodontal disease and tooth loss. Dental caries is a multifunctional disease in which diet, nutrition, microbial infection and host response play important roles. It has been shown that human salivary amylase (HSA) takes part in the formation of dental plaque and subsequent caries formation. In solution α-amylase binds with high affinity to viridans oral *Streptococci*. The bacteria-bound amylase is capable of hydrolyzing starch to oligosaccharides, which can be used as a food source by the bacteria where it is metabolized to lactic acid. The local acid production can lead to the dissolution of tooth enamel, which is a critical step in dental caries progression;[1,2] as such inhibition of HSA could decrease the risk of caries formation.

α-Amylase inhibitors are diverse as they can be synthetic, microbial and of plant origin. Tannins are natural polyphenolic compounds of high molecular weight, which form insoluble complexes with proteins. According to their chemical structures tannins are subdivided into two groups: hydrolyzable and condensed. Hydrolyzable tannins are molecules with a polyhydroxy component, generally D-glucose, as a central core. The hydroxyl groups of these molecules are partially or totally esterified with phenolic compounds, such as gallic acid (gallotannins) or ellagic acid (ellagitannins).[3,4]

The antimicrobial effects of tannins have been widely recognized. Kakiuchi and co-workers[5] have studied several traditional Chinese medicines for antibacterial activity against *Streptococcus mutans*, a primary cariogenic bacterium. Gallotannin-rich extracts inhibited the adherence of *S. mutans* to smooth surfaces.[6]

* Corresponding author. Fax: +36 52 512 913; e-mail: kandra@puma.unideb.hu

0008-6215/$ - see front matter © 2006 Elsevier Ltd. All rights reserved.
doi:10.1016/j.carres.2006.12.016

The tannins have general protein complexing properties, which can cause variable enzyme inhibition. For example, teaflavins and galloylated flavan-3-ols are known to have antiglucosyltransferase activity.[7] The inhibitory effects of hydrolyzable and condensed tannins,[8] polyphenols and tannins from *Larix laricina*[9] were investigated on xanthine oxidase. Ellagitannins proved to be potent inhibitors of protein kinase C.[10] Proantocyanidins have inhibiting properties on the angiotensin I-converting enzyme (ACE).[6] It is also known that tea polyphenols have, amongst others, inhibitory effect on salivary α-amylase.[11] Very recently, soft fruit extracts (rich in ellagitannins and anthocyanins) were found to be effective α-amylase inhibitors.[12] The exact structure of active tea polyphenols and kinetic properties of tea and fruit extracts have not yet been investigated.

The three-dimensional structure of HSA was described by Ramasubbu and co-workers.[13] HSA consists of three domains where the domain A adopts the $(\beta/\alpha)_8$ barrel structure bearing three catalytic residues Asp197, Glu233 and Asp300. The active site of HSA is present in domain A as a deep, V-shaped cleft and it harbours aromatic residues, which provide stacking interactions to the bound glucose moieties. The role of aromatic residues in the active centre was studied by mutational and subsite mapping analysis previously in this laboratory.[14,15]

In this paper, we report the kinetic investigation of a natural amylase inhibitor, a tannin isolated from the gall nut of Aleppo oak, on the HSA-catalyzed hydrolysis of a synthetic and a natural substrate.

2. Results and discussion

2.1. Structural characterization of Aleppo tannin

The structural parameters of tannin were established by gallic acid determination with rhodanine, by the measurement of ellagic acid amount with the nitrite assay, and by ESIMS.

Gallic acid is present in two forms in plants, as an ester (with different types of polyhydroxy compounds) and as a free acid. As such, two separate assays were necessary to determine the form of the tannin. One was performed before the hydrolysis to quantify the free gallic acid (3%) and the second after acid hydrolysis to quantify total gallic acid (70%). Similarly, in order to determine free (2%) and total ellagic acid (7%), two assays were performed, before and after hydrolysis. The proportions of gallic and ellagic acid were compared to the amount of tannin in the reaction mixture.

The electrospray mass spectrometry analysis was carried out in negative ion mode. In the spectrum, five peaks are present (Fig. 1).

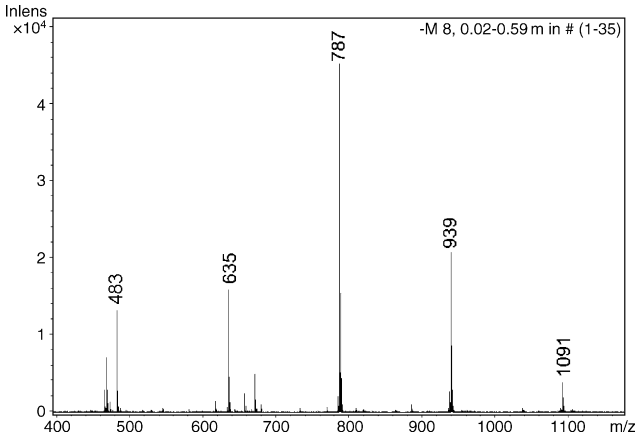

Figure 1. ESI mass spectrum of Aleppo tannin.

Their molecular weights differ from each other by 152 mass units, which is equivalent to the molecular mass of a galloyl moiety. These data and the molecular masses, represented by the peaks, suggest that the structure of Aleppo tannin is based on glucose, which is esterified with 2–6 gallic acids. The peaks at m/z 483.088; 635.100; 787.113; 939.127; and 1091.142 Da belong to the deprotonated $[M-H]^-$ form of digalloyl-, trigalloyl-, tetragalloyl-, pentagalloyl- and hexagalloyl-glucose, respectively.

The $[M-H]^-$ ions were observed in negative mode measurements and the ionization properties of ellagi- and gallotannins were the same because of their similar structures.

However, there are some peaks in the spectrum with low intensities (<10%), which have not been identified. At the time of writing Aleppo tannin has not been analyzed by mass spectrometry, but different gallotannins and ellagitannins have been characterized from longan seed[16] and carob fibre[17] using ESIMS and HPLC-ESIMS methods, respectively.

These results confirm that Aleppo tannin is a gallotannin, in which the glucose core is di- up to hexagalloylated and the mixture also contains 7% ellagic acid. The calculated average molecular mass (M_n) of Aleppo tannin is 763 Da.

2.2. Inhibition studies

The inhibition kinetics were analyzed using Lineweaver–Burk, Dixon plots and the corresponding secondary plots. Initial velocities were determined by spectrophotometry at different substrate concentrations in the presence and absence of fixed inhibitor concentrations. Figures 2 and 3 show the Lineweaver–Burk plots for the Aleppo tannin inhibited hydrolysis of $GalG_2$-CNP and amylose substrates in the presence of HSA. Replots of the slopes (s) and the vertical axis intercepts (i) versus the inhibitor concentrations are also presented.

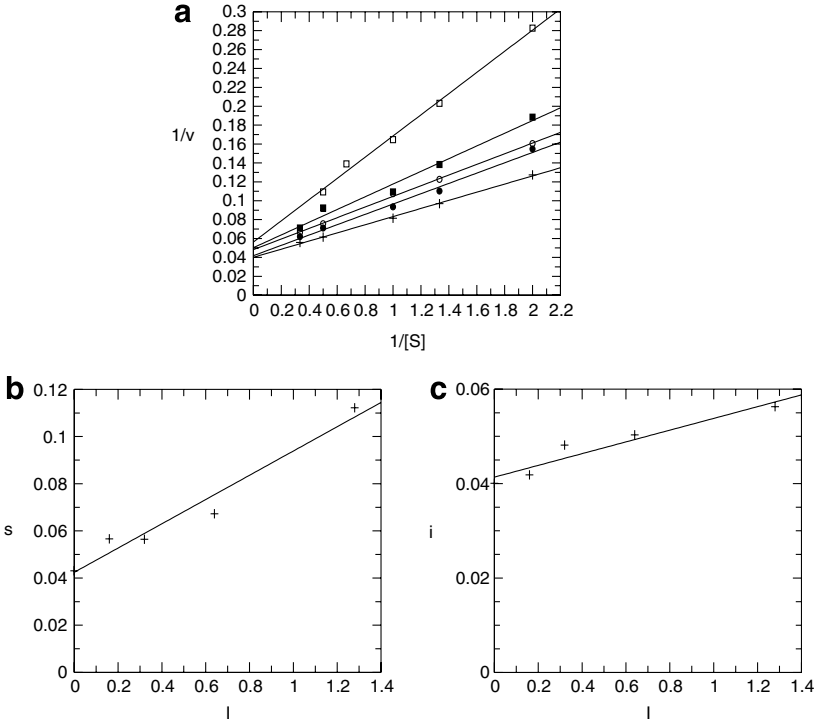

Figure 2. Lineweaver–Burk plots (a) and secondary plots (b) slope (*s*) versus [I], (c) intercept (*i*) versus [I]. Reciprocal plots obtained with variable $GalG_2$-CNP concentrations (mM) at fixed tannin concentrations: +, 0 μg mL^{-1}; ●, 0.16 μg mL^{-1}; ○, 0.32 μg mL^{-1}; ■, 0.64 μg mL^{-1}; □, 1.28 μg mL^{-1}. 1/*v* values are given as μmol min^{-1}.

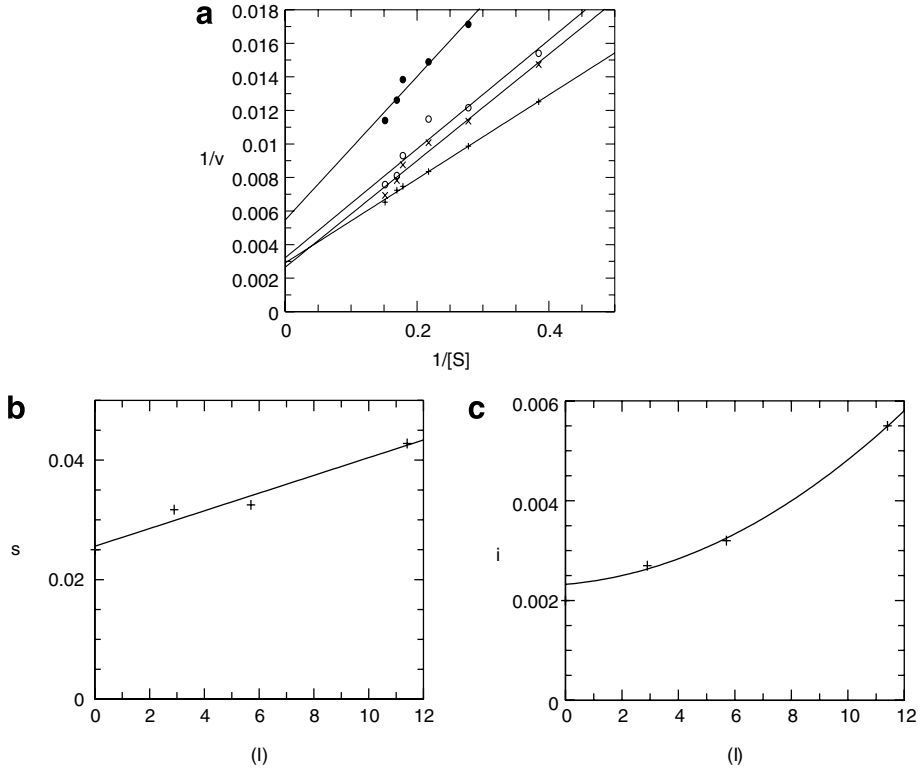

Figure 3. Lineweaver–Burk plots (a) and secondary plots (b) slope and (*s*) versus [I], (c) intercept (*i*) versus [I]. Reciprocal plots obtained with variable amylose concentrations (mg mL^{-1}) at fixed tannin concentrations: +, 0 μg mL^{-1}; ×, 2.9 μg mL^{-1}; ○, 5.7 μg mL^{-1}; ●, 11.4 μg mL^{-1}. 1/*v* values are given as μmol min^{-1}.

In both cases, the primary plots give straight lines (Figs. 2a and 3a). Both the slope (s) and the vertical axis intercept (i) increase with increasing tannin concentration. These results account for a mixed type of inhibition.

Plotting the slopes (s) and the vertical axis intercepts (i) against the tannin concentration, respectively, produced straight lines (Fig. 2b and c) in the case of the short, chromogenic substrate.

First order equations 3 and 4 (given in Section 3) of these lines with respect to the tannin concentration indicate that one inhibitor molecule binds either to the free enzyme or to the enzyme–substrate complex.

However, when amylose was used as a substrate the analysis of secondary plots intercept versus inhibitor concentration gave different results, and curved lines with an upward concavity were obtained (Fig. 3c).

The $s = f_{([I])}$ is first order, which indicates that only one inhibitor molecule binds to the free enzyme. The second order relation between the tannin concentration and intercept suggests the binding of two molecules of inhibitor to the ES complex (Eq. 5).

2.3. Discussion

The K_{EI} and K_{ESI} dissociation constants were calculated from the Lineweaver–Burk secondary plots using the Grafit program and are displayed in Table 1.

In the case of $GalG_2$-CNP substrate, the lower value of K_{EI} indicates a more favourable formation of EI than ESI complex. For the amylose substrate, the values of K_{ESI} and K_{ESI_2} are comparable with the value of K_{EI}, indicating that there is almost an equal probability of EI, ESI and ESI_2 complexes to form. As such, inhibition is unambiguously of a mixed type.

Tannins are used for the extraction of mucilaginous polysaccharides (e.g., the acetylated mannan in aloe, glucans produced by plants or by cultured microorganisms) from aqueous extracts by complexation.[18] It is also reported that, among other polysaccharides, amylose can develop secondary structures containing hydrophobic cavities, and associate strongly with polyphenolic compounds.[19]

These results suggest that Aleppo tannin can interact also with the amylose substrate. It is presumed that with increasing inhibitor concentration, the type of inhibition can change. In the case of amylase, the Lineweaver–Burk plots show competitive-like inhibition at low inhibitor levels and non-competitive-like inhibition at high inhibitor concentrations. In the case of competitive inhibition, galloylated glucose binds to the active site of HSA and interacts with the known aromatic residues of the enzyme or forms hydrogen bonds with subsite residues. When the inhibition is non-competitive, the inhibitor can bind either to the secondary site of the enzyme or to the substrate in the enzyme–substrate complex.

The binding of the inhibitor is significantly affected by the type of substrate used in this study. When $GalG_2$-CNP was the substrate, the binding of the inhibitor probably occurs at the active site of the enzyme. In the case of amylase, the mechanism of inhibition is somewhat different. One inhibitor molecule binds to the free enzyme and two inhibitors bind to the enzyme–substrate complex. Presumably one inhibitor molecule binds to the secondary site of the enzyme and the other one binds to the amylose substrate in the ESI_2 complex.

Aleppo tannin turned out to be a better inhibitor when the short $GalG_2$-CNP substrate was used, as compared to the long-chain amylose. A marked difference was observed, especially for the competitive constant, where the K_{EI} value is twelve times higher for the amylose substrate. However, the uncompetitive constant (K_{ESI}) for amylose is only about five times higher. Changing the type of substrate makes a difference in the way the ESI_2 complex is formed, which may probably be explained by the interaction between the inhibitor and amylose. In the case of the $GalG_2$-CNP substrate, the relationship between inhibitor concentration and the intercept is linear but not in the presence of amylose. Since the two kinetic measurements differ from each other only in the substrates used (size, structure), the difference in the inhibition kinetics can be explained by the binding of tannin to the amylose substrate. Previously, kinetic measurements on $GalG_2$-CNP substrate were carried out in our laboratory with a gallotannin. This was a mixture containing di- up to heptagalloylated quinic acid molecules. The dissociation constants (K_{EI} 9.0 μg mL^{-1}, K_{ESI} 47.9 μg mL^{-1}) were one order of magnitude higher than in the case of the Aleppo tannin under the same experimental conditions using the $GalG_2$-CNP substrate.[20]

These results show that Aleppo oak tannin has even better inhibitory effect on HSA than earlier investigated tannin and the kinetic constants are closer to the values obtained using acarbose (K_{EI} 0.45 μg mL^{-1}, K_{ESI} 0.065 μg mL^{-1}) measured on $GalG_2$-CNP hydrolysis.[21]

Table 1. Kinetic constants of HSA-catalyzed hydrolysis in the presence of Aleppo tannin

Substrate	Kinetic constants		Dissociation constants[a]		
	K_M	v_{max} (μmol min^{-1})	K_{EI} (μg mL^{-1})	K_{ESI} (μg mL^{-1})	K_{ESI_2} (μg mL^{-1})
$GalG_2$-CNP	0.9 mM	21.4	0.82	3.32	—
Amylose	10.6 mg mL^{-1}	416	17.4	14.86	9.64

[a] Dissociation constants are given in μg mL^{-1} since the exact molecular mass cannot be calculated.

MALDI-TOFMS post source decay analysis is in progress to find structural explanation for these results. Because of the good inhibitory potential of tannin on HSA, in vivo experiments are planned to test the benefit of Aleppo tannin for the prevention of dental caries.

3. Experimental

3.1. Materials

3.1.1. Substrates. Kinetic studies were carried out on both a synthetic chromogenic substrate 2-chloro-4-nitrophenyl 4-*O*-β-D-galactopyranosyl-α-maltoside ($GalG_2$-CNP from SORACHIM S.A.) and the natural substrate amylose (from GENAY). $GalG_2$-CNP is a well-known and general substrate – especially in clinical chemistry – for amylase activity measurements. This substrate requires no auxiliary enzyme to release the chromophore, since it is exclusively cleaved at the aglycone bond resulting in only two degradation products; β-D-galactopyranosyl-maltose and 2-chloro-4-nitrophenol (CNP). No other fragment is produced.[22] The released chromophore can be detected at 405 nm. For the selective cleavage of CNP, the addition of 152 mM azide is necessary. The structural formula of $GalG_2$-CNP is shown in Figure 4.

Since the size and structure of $GalG_2$-CNP are different from the natural substrate of amylases, it is interesting to compare the kinetic parameters for both substrates.

3.1.2. Enzyme. α-Amylase (EC 3.2.1.1) from human saliva (Type IXA Sigma) gave a single band on sodium dodecyl sulfate-polyacrylamide gel electrophoresis (SDS-PAGE) and possessed no α- and β-glycosidase activity.

3.1.3. Inhibitor. Tannin isolated from the gall nut of Aleppo oak (gallae halepenses) was obtained from Biotechnology Services and Consulting Inc., Coppell, USA.[18] Extraction was carried out at room temperature with 60% aq acetone. The commercial Aleppo tannin was further purified by size exclusion chromatography using a Sephadex LH-20 column, following the usual techniques for gallotannins.[23] The structural characterization of tannin was based on the determination of gallotannin, ellagitannin and by ESIMS analysis. The chemical analysis revealed the presence of 3%, 70%, 2% and 7% free and bound gallic and ellagic acid, respectively. Our findings are consistent with the chemical content of Aleppo gall, that is, 2%, 65%, 0%, and 2% free and bound gallic and ellagic acid, respectively.[24]

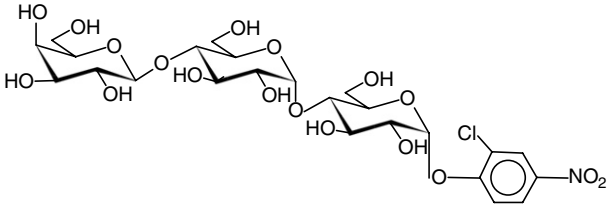

Figure 4. Structure of $GalG_2$-CNP.

3.2. Gallic acid determination

The gallic acid-content was determined by the rhodanine method of Hagerman and Inoue.[25] Rhodanine reacts with the vicinal hydroxyl groups of gallic acid to give a red complex with a maximum absorbance at 520 nm. The unreacted rhodanine, under the basic conditions of the test, has maximum absorbance at 412 nm with no absorbance at wavelengths higher than 450 nm. The red colour is formed with free gallic acid and not with gallic acid esters, ellagic acid or other phenolic components that may be present in the extract. Gallic acid was used as a standard and the results were based on experiments carried out in triplicate. The measured absorbance obeys the linear relationship: $A_{520} = [0.1562\ (\mu g\ mL^{-1}$ of gallic acid)]. The method was described in detail in an earlier publication.[20]

The hydrolysis must be carried out anaerobically to prevent destructive oxidation. The hydrolysis tubes were sealed under vacuum, which is a simple and reliable method for anaerobic hydrolysis.

3.3. Ellagic acid determination

The ellagic acid-content was measured by the method of Hagerman and Wilson.[26] The spectrophotometric method for the determination of ellagic acid is based on the formation of a red quinone oxime of the ellagic acid nitrosylation product (electrophilic aromatic substitution). The colour is produced by reacting the sample at 30 °C with sodium nitrite in pyridine, using HCl as a catalyst. This method is selective, giving a positive reaction for free ellagic acid but not for numerous other common plant phenolics, including gallic acid, ellagic acid esters, pro-anthocyanidins and flavonoids. The method was standardized with commercial ellagic acid. Samples (10 mg) of tannin in 1 M H_2SO_4 (1 mL) were put into constricted test tubes and frozen. The tubes were sealed under vacuum and heated for 24 h at 100 °C before being cooled and opened. Filtered content was made up to 10.0 mL with pyridine. Then 1.1 mL of pyridine and 1 mL of the sample were mixed in a dry test tube. After adding 0.10 mL of concentrated HCl and mixing, the sample was brought to 30 °C. The sample was quickly mixed after the addition of 0.10 mL of 1% (w/v) $NaNO_2$ in water, and the absorbance was immediately recorded at 538 nm. After a 36 min incubation period at 30 °C, the absorbance was measured again. The

difference between the initial absorbance and the absorbance at 36 min (ΔA_{538}) was proportional to the ellagic acid concentration. The measured absorbance obeys the relationship: $A_{538} = [0.03\ (\text{mg of ellagic acid})] - 0.04$.

3.4. Mass spectrometry

Negative ESIMS was recorded using a Bruker micro-TOF-Q mass spectrometer. The instrumental parameters were as follows: scan range m/z 50–3000, dry gas nitrogen, temperature 150 °C, reflector voltage 1300 V, detector voltage 1920 V. The sample in 1:1 MeOH–water (0.1 mg mL^{-1}) was infused at a flow rate of 2 μL min^{-1}. External calibration was applied using the $[M-H]^-$ peaks of sodium trifluoroacetate cluster ions in a mass range of 200–1200 Da.

3.5. Kinetic studies on $GalG_2$-CNP

Measurements using the short, chromogenic substrate were carried out at 37 °C in 50 mM MES buffer, pH 6.0, containing 5 mM $Ca(OAc)_2$, 51.5 mM NaCl and 152 mM of sodium azide. The substrate (0.5–3 mM) and inhibitor (0.16–1.28 μg mL^{-1}) were mixed and the reaction was initiated by adding HSA (2 nM) to the incubation medium, to a final vol of 500 μL. We controlled the inhibitor, Aleppo tannin, so that it is not cleaved under the kinetic experimental conditions. The increase in absorbance arising from the HSA-liberated CNP was measured continuously at 400 nm using the Parallel Kinetics Analysis program of a JASCO V550 spectrophotometer. The initial velocity was determined from the slope of the linear part of the kinetic curves. All experiments were repeated three to four times.

3.6. Kinetic studies on amylose using the dinitrosalicylic acid method[27]

Kinetic analysis was carried out at 37 °C in phosphate buffer, pH 7, containing 48.6 mM Na_2HPO_4, 38.8 mM KH_2PO_4 and 50 mM NaCl. The substrate (2.6–6.6 mg mL^{-1}) and inhibitor (2.9–11.4 μg mL^{-1}) were mixed together and the reaction was initiated by adding amylase (6.5 nM) to the incubation medium to a final vol of 150 μL. After 10 min, the reaction was quenched by adding 1 mL of dinitrosalicylic (DNS) reagent (1% 3,5-dinitrosalicylic acid, 0.2% phenol, 0.1% Na_2SO_3, 1% aq NaOH). The resulting soln was made up to 2 mL using phosphate buffer. The capped test tubes were then heated at 100 °C for 15 min to develop the yellow-brown colour. Afterwards 300 μL of a 40% potassium sodium tartrate (Rochelle salt) soln was added to the test tubes to stabilize the colour. After cooling to room temperature, in a cold water bath, the absorbance was recorded at 540 nm using the Fixed Wavelength Measurement program of a JASCO V550 spectrophotometer.

3.7. Statistical analysis

The type of inhibition was determined by the Lineweaver–Burk plot, and its replots of slopes and vertical axis intercepts versus inhibitor concentration. A general scheme of possible formation of inhibitor complexes is presented in Figure 5.

The general equations for the kinetic analysis in the case of $GalG_2$-CNP and amylose substrate are Eqs. 1 and 2, respectively

$$v_0 = \frac{v_{\max}[S]}{K_M\left(1+\frac{1}{K_{EI}}[I]\right)+[S]\left(1+\frac{1}{K_{ESI}}[I]\right)} \quad (1)$$

$$v_0 = \frac{v_{\max}[S]}{K_M\left(1+\frac{[I]}{K_{EI}}\right)+[S]\left(1+\frac{[I]}{K_{ESI}}+\frac{[I]^2}{K_{ESI}K_{ESI_2}}\right)} \quad (2)$$

The equations for Lineweaver–Burk secondary plots are given by Eqs. 3–5

$$s = \frac{K_M}{v_{\max}} + \frac{K_M}{v_{\max}K_{EI}}[I] \quad (3)$$

$$i = \frac{1}{v_{\max}} + \frac{1}{v_{\max}K_{ESI}}[I] \quad (4)$$

$$i = \frac{1}{v_{\max}} + \frac{1}{v_{\max}K_{ESI}}[I] + \frac{1}{v_{\max}K_{ESI}K_{ESI_2}}[I]^2 \quad (5)$$

Eqs. 3 and 4 describe the relation of Figure 2b and c, respectively, while Eqs. 3 and 5 correspond to Figure 3b and c, respectively.

The symbols of the equations are as follows: v_0 is the initial velocity in the absence and presence of the inhibitor, $v_{\max}$ is the limiting velocity, [S] and [I] are the concentrations of the substrate and the inhibitor, K_M is the Michaelis-constant, K_{EI}, K_{ESI} and K_{ESI_2} are the dissociation constants of the inhibitor containing complexes EI, ESI, and ESI_2, respectively. Eqs. 3–5 were applied for the calculation of inhibition constants from the secondary plots of Lineweaver–Burk linearization.

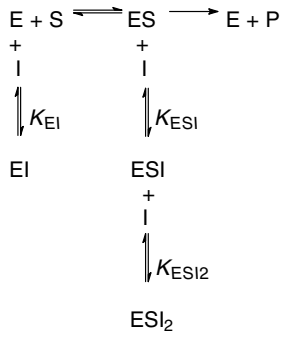

Figure 5. Presentation of different enzyme–inhibitor complexes and kinetic constants of the kinetic equations 1–5.

Acknowledgement

This work was supported by grants from the Hungarian Scientific Research Fund (OTKA T047075, T043399).

References

1. Scannapieco, F. A.; Torres, G. I.; Levine, M. J. *J. Dent. Res.* **1995**, *74*, 1360–1366.
2. Scannapieco, F. A.; Bergey, E. J.; Reddy, M. S.; Levine, M. J. *Infect. Immun.* **1989**, *57*, 2853–2863.
3. www.ansci.cornell.edu/plants/toxicagents/tannin.
4. www.users.muohio.edu/hagermae.
5. Kakiuchi, N.; Hattori, M.; Nishizawara, M.; Yamagishi, T.; Okuda, T.; Namba, T. *Chem. Pharm. Bull.* **1986**, *34*, 720–725.
6. Buryne, T. D.; Pieters, L.; Deelstra, H.; Vlietink, A. *Biochem. Syst. Ecol.* **1999**, *27*, 445–459.
7. Hattori, M.; Kusumoto, I.; Namba, T.; Ishigami, T.; Hara, Y. *Chem. Pharm. Bull.* **1990**, *38*, 717–720.
8. Hatano, T.; Yashuhara, T.; Yoshihara, R.; Agata, I.; Voro, T.; Okuda, T. *Chem. Pharm. Bull.* **1990**, *38*, 1224–1229.
9. Owen, P. L.; Johns, T. *J. Ethnopharmacol.* **1999**, *64*, 149–160.
10. Kashiwada, Y.; Nonaka, G.; Nishioka, I.; Ballas, L. M.; Jiang, J. B.; Janzen, W. P.; Lee, K.-H. *Bioorg. Med. Chem. Lett.* **1992**, *2*, 239–244.
11. Zhang, J.; Kashket, S. *Caries Res.* **1998**, *32*, 233–238.
12. McDougall, G. J.; Shpiro, F.; Dobson, P.; Blake, A.; Stewart, D. *J. Agric. Food Chem.* **2005**, *53*, 2760–2766.
13. Ramasubbu, N.; Paloth, V.; Luo, Y.; Brayer, G. D.; Levine, M. J. *Acta Crystallogr., Sect. D* **1996**, *52*, 435–446.
14. Kandra, L.; Gyémánt, G.; Remenyik, J.; Ragunath, C.; Ramasubbu, N. *FEBS Lett.* **2003**, *544*, 194–198.
15. Ramasubbu, N.; Ragunath, C.; Mishra, P. J.; Thomas, L. M.; Gyémánt, G.; Kandra, L. *Eur. J. Biochem.* **2004**, *271*, 2517–2529.
16. Soong, Y. Y.; Barlow, P. J. *J. Chromatogr., A* **2005**, *1085*, 270–277.
17. Owen, R. W.; Haubner, R.; Hull, W. E.; Erben, G.; Spiegelhalder, B.; Bartsch, H.; Haber, B. *Food Chem. Toxicol.* **2003**, *41*, 1727–1738.
18. Vittori, N. U.S. Patent 6,482,942, 2000; *Chem. Abstr.* **2000**, *133*, 101738s.
19. Ozawa, T.; Lilley, T. H.; Haslam, E. *Phytochemistry* **1987**, *26*, 2937–2942.
20. Kandra, L.; Zajácz, Á.; Remenyik, J.; Gyémánt, G. *Biochem. Biophys. Res. Commun.* **2004**, *319*, 1265–1271.
21. Kandra, L.; Zajácz, Á.; Remenyik, J.; Gyémánt, G. *Biochem. Biophys. Res. Commun.* **2005**, *334*, 824–828.
22. Morishita, Y.; Iinuma, Y.; Nakashima, N.; Majima, K.; Mizuguchi, K.; Kawamura, Y. *Clin. Chem.* **2000**, *46*, 928–933.
23. Hagerman, A. E. *J. Chem. Ecol.* **1988**, *14*, 453–461.
24. Fagan, M. M. *Am. Nat.* **1918**, *52*, 155–176.
25. Hagerman, A. E.; Inoue, K. H. *Anal. Biochem.* **1988**, *169*, 363–369.
26. Hagerman, A. E.; Wilson, T. C. *J. Agric. Food Chem.* **1990**, *38*, 1678–1683.
27. Miller, G. L. *Anal. Chem.* **1959**, *31*, 426–428.